



HAL
open science

Nature and relationships of *Sahelanthropus tchadensis*

Roberto Macchiarelli, Aude Bergeret-Medina, Damiano Marchi, Bernard Wood

► **To cite this version:**

Roberto Macchiarelli, Aude Bergeret-Medina, Damiano Marchi, Bernard Wood. Nature and relationships of *Sahelanthropus tchadensis*. *Journal of Human Evolution*, 2020, 149, pp.102898. 10.1016/j.jhevol.2020.102898 . hal-03349899

HAL Id: hal-03349899

<https://hal.science/hal-03349899>

Submitted on 7 Nov 2022

HAL is a multi-disciplinary open access archive for the deposit and dissemination of scientific research documents, whether they are published or not. The documents may come from teaching and research institutions in France or abroad, or from public or private research centers.

L'archive ouverte pluridisciplinaire **HAL**, est destinée au dépôt et à la diffusion de documents scientifiques de niveau recherche, publiés ou non, émanant des établissements d'enseignement et de recherche français ou étrangers, des laboratoires publics ou privés.



Distributed under a Creative Commons Attribution - NonCommercial 4.0 International License

1 Nature and relationships of *Sahelanthropus tchadensis*

2

3 Roberto Macchiarelli ^{a, b, *}, Aude Bergeret-Medina ^c, Damiano Marchi ^{d, e}, Bernard Wood ^f

4

5 ^a *Unité de Formation Géosciences, Université de Poitiers, 86073 Poitiers, France*

6 ^b *Département Homme & Environnement, UMR 7194 CNRS, Muséum national d'Histoire*
7 *naturelle, 75116 Paris, France*

8 ^c *448C, Chemin de Souilles, 82410 Saint-Etienne-de-Tulmont, France*

9 ^d *Department of Biology, University of Pisa, 56126 Pisa, Italy*

10 ^e *Evolutionary Studies Institute and Centre for Excellence in Palaeosciences, University of the*
11 *Witwatersrand, Wits 2050, South Africa*

12 ^f *Center for the Advanced Study of Human Paleobiology and Department of Anthropology,*
13 *George Washington University, Washington, DC 20052, USA*

14

15

16 * Corresponding author.

17 *E-mail address:* roberto.macchiarelli@univ-poitiers.fr (R. Macchiarelli).

18

19 **Acknowledgments**

20 This contribution benefited from data and interpretations made by L. Puymerau on CT scans
21 of BAR 1002'00 and BAR 1003'00 kindly made available by B. Senut and M. Pickford. For
22 access to comparative materials, scanning facilities, and/or data/information sharing, we
23 acknowledge S. Almécija, A. Beauvilain, D.R. Begun, B. Billings, L. Bondioli, J. Braga, M.

24 Cazenave, J. Chupasko, F. de Beer, J.M. DeSilva, M. Domínguez-Rodrigo, Y. Haile-Selassie, K.
25 Jakata, L. Jellema, J.W. Kappelman, L. Kgasi, T.L. Kivell, E. L'Abbé, I. Livne, R. Martin, B.
26 Martínez-Navarro, M. Nakatsukasa, S. Peigné, M. Pina, S. Potze, L. Rook, C.B. Ruff, L. Salzani,
27 M.M. Skinner, J.-F. Tournepiche, E. Westwig, C. Zanolli, and B. Zipfel. We also acknowledge
28 the Institut Català de Paleontologia Miquel Crusafont, the Digital Morphology Museum (KUPRI,
29 <http://dmm.pri.kyoto-u.ac.jp/dmm/WebGallery/index.html>) and the MorphoSource
30 (<https://www.morphosource.org/>) for access to their 3D databases. The input from three
31 reviewers, two Associate Editors and two Editors was greatly appreciated.

32

1 Nature and relationships of *Sahelanthropus tchadensis*

2

3 *Keywords:* Hominid; Hominin; *Sahelanthropus tchadensis*; Femur

4

5 ABSTRACT

6

7 A partial left femur (TM 266-01-063) was recovered in July 2001 at Toros-Menalla, Chad, at the
8 same fossiliferous location as the late Miocene holotype of *Sahelanthropus tchadensis* (the
9 cranium TM 266-01-060-1). It was recognized as a probable primate femur in 2004, when one of
10 the authors was undertaking a taphonomic survey of the fossil assemblages from Toros-Menalla.
11 We are confident the TM 266 femoral shaft belongs to a hominid. It could sample a hominid
12 hitherto unrepresented at Toros-Menalla, but a more parsimonious working hypothesis is that it
13 belongs to *S. tchadensis*. The differences between TM 266 and the late Miocene *Orrorin*
14 *tugenensis* partial femur BAR 1002'00, from Kenya, are consistent with maintaining at least a
15 species-level distinction between *S. tchadensis* and *O. tugenensis*. The results of our preliminary
16 functional analysis suggest the TM 266 femoral shaft belongs to an individual that was not
17 habitually bipedal, something that should be taken into account when considering the
18 relationships of *S. tchadensis*. The circumstances of its discovery should encourage researchers
19 to check to see whether there is more postcranial evidence of *S. tchadensis* among the fossils
20 recovered from Toros-Menalla.

21

22 **1. Introduction**

23

24 There are now several lines of evidence—morphological, molecular and genetic—to support
25 the hypothesis that the living taxa most closely related to modern humans are chimpanzees and
26 bonobos (Ruvolo, 1997; Prado-Martinez et al., 2013; Diogo et al., 2017). Most attempts to
27 calibrate the DNA differences suggest the human (hominin) lineage has been separate from the
28 *Pan* (panin) lineage for ca. 8–6 Myr (Bradley, 2008; Stone et al., 2010), but extrapolations based
29 on generation times in *Pan* and *Gorilla* (Langergraber et al., 2012; see also Moorjani et al., 2016)
30 suggest the divergence date may be earlier. Two putative hominin taxa are known from ca. 8–6
31 Ma in Africa. One, *Orrorin tugenensis*, was established to accommodate dental and postcranial
32 remains recovered from ca. 6.0 Ma Lukeino Formation sediments exposed at Aragai, Cheboit,
33 Kapcheberek and Kapsomin in the Baringo District, Kenya (Senut et al., 2001). This contribution
34 focuses on the other taxon, *Sahelanthropus tchadensis*, which was established to accommodate
35 fossil remains from Chad (Brunet et al., 2002).

36 The first published evidence for *S. tchadensis* consisted of six fossils—including the holotype
37 specimen, an adult cranium (TM 266-01-060-1, hereafter the TM 266 cranium)—all of which
38 were recovered from a single locality, TM 266, in the informal 'anthracotheriid unit' at Toros-
39 Menalla (Brunet et al., 2002). Additional specimens recovered in 2001 and 2002, including an
40 upper premolar tooth from TM 266, and two mandibles, TM 247-01-02 and TM 292-02-01
41 (Brunet et al., 2005), are consistent with the hypothesis that a single species was represented in
42 these collections. Currently described remains assigned to *S. tchadensis* sample from six to nine
43 adult individuals from three fossiliferous localities (TM 247, 266 and 292) scattered across ca.
44 0.73 km² (Brunet et al., 2002, 2005). Cosmogenic nuclide (¹⁰Be/⁹Be) dating methods suggest that

45 the Toros-Menalla localities are older than 6.83 ± 0.45 Ma and younger than 7.04 ± 0.18 Ma
46 (Lebatard et al., 2008), which would place them at the older end of the biochronology-derived
47 ca. 7–6 Ma range (Vignaud et al., 2002). The cosmogenic nuclide ages assume the fossils were
48 found in situ in the sediments. Brunet et al. (2004) implied that part of the holotype cranium was
49 still partly buried when it was discovered, but this has been disputed by Beauvilain and Watté
50 (2009).

51 The cranium of *S. tchadensis*, while relatively complete, is distorted, and many areas are
52 permeated by matrix-filled cracks. Nonetheless, what is preserved displays a novel combination
53 of primitive (i.e., African ape-like) and derived (i.e., later hominin-like) features (Guy et al.,
54 2005). Much about the cranial base and neurocranium, including its estimated endocranial
55 volume (360–370 cm³; Zollikofer et al., 2005), is African ape-like, as is the subocclusal
56 mandibular dental morphology (Emonet et al., 2014). Notable exceptions in the cranium are the
57 supraorbital torus, the more horizontal nuchal plane, and the location of the foramen magnum.
58 Although in its recovered state the foramen magnum of the TM 266 cranium is more anteriorly
59 placed than is generally the case in chimpanzees, it is located in the zone of overlap between the
60 ranges for bonobos and modern humans (Ahern, 2005). The presence of a supraorbital torus
61 integrated into the cranial vault, combined with a relatively flat lateral profile of the face, small,
62 apically-worn canines, molar teeth with low, rounded cusps and relatively thick enamel, and a
63 relatively thick mandibular corpus, were all cited by its discoverers as features that excluded *S.*
64 *tchadensis* from any close relationship with the *Pan* clade (Brunet et al., 2002; Guy et al., 2005).

65 Zollikofer et al. (2005) attempted to overcome the problems posed by the distortion and
66 matrix-filled cracking by applying the techniques of virtual reconstruction—images based on CT
67 scans manipulated using sophisticated computer software—to the TM 266 cranium. They

68 claimed that the virtually-reconstructed cranium strengthened the case for *S. tchadensis* being an
69 early hominin by showing that it requires substantial adjustments in multidimensional size–shape
70 space to transform TM 226 into either a *Pan*-like, or a *Gorilla*-like, cranium (Zollikofer et al.,
71 2005: Fig. 3). They also used “minimum form change” (Zollikofer et al., 2005: 755) as evidence
72 to refute the hypothesis that *S. tchadensis* is a fossil gorillin (Wolpoff et al., 2002, 2006).
73 However, if we accept their use of relative “minimum form change” as a taxonomic
74 discriminator, then it would self-evidently involve even more substantial adjustments in
75 multidimensional size–shape space to convert the TM 266 cranium into a modern human
76 cranium, so if we use the same logic Zollikofer et al. (2005) used to argue the TM 266 cranium
77 was not that of a fossil gorillin, then it is even less likely to be a hominin. When Guy et al.
78 (2005) used 3D geometric morphometric landmark-based methods to capture and compare the
79 morphology of the TM 266 cranium with extant and fossil taxa, their assessment of the
80 implications of the virtually-reconstructed cranium was more nuanced. While they stated that
81 “*Sahelanthropus tchadensis* is clearly a hominid” (a hominin in our usage; Guy et al., 2005:
82 18840), they also acknowledged that some aspects of its cranial morphology such as the
83 “anteroinferiorly sloping midfacial contour in the midsagittal plane” and “shortened rostrum with
84 substantial projection of the upper face relative to the neurocranium” (Guy et al., 2005: 18838),
85 are either novel morphological features, or novel combinations of features, and they also
86 cautioned that some similarities with fossil hominins, such as the features the TM 266 cranium
87 shares with KNM-ER 1813, could be “either primitive or convergent with *Homo*” (Guy et al.,
88 2005: 18839). In the virtually rendered TM 266 cranium it is noteworthy that the reconstructed
89 angle between the foramen magnum and the orbital plane is closer to the values typical of *Homo*
90 *sapiens* than to those of australopiths (Zollikofer et al., 2005: Fig. 4). In a recent phylogenetic

91 analysis using an updated version of the craniodental character matrix used by Strait and Grine
92 (2004), Mongle et al. (2019) concluded that the bootstrap support for *S. tchadensis* being a
93 hominin was absolutely low (41%), and relatively low compared to the bootstrap support for
94 *Ardipithecus ramidus* (64%).

95 So, given the difficulties of inferring the characteristic morphology of a taxon with a
96 relatively meager fossil record (Smith, 2005), and the fact that the nature and relationships of *S.*
97 *tchadensis* rely on morphological evidence from a distorted cranium, or from a virtually-
98 reconstructed version of that cranium, any additional information, especially from anatomical
99 regions not sampled in the existing hypodigm, has the potential to help clarify the evolutionary
100 relationships of *S. tchadensis*. Specifically, the current hypodigm of *S. tchadensis* does not
101 include any postcranial remains that might be informative about the posture and locomotion of *S.*
102 *tchadensis* (Brunet et al., 2002, 2004, 2005; Brunet and Jaeger, 2017). The purpose of this
103 contribution is to introduce the first postcranial evidence of *S. tchadensis*.

104

105 1.1. *The partial femur TM 266-01-063*

106

107 According to Beauvilain and Watté (2009), a partial left femur (TM 266-01-063, hereafter the
108 TM 266 femur) was collected on 19th July 2001 at locality TM 266 (16°15'12" N; 17°29'29" E)
109 in the same location as the holotype TM 266 cranium. It was recognized as a probable primate
110 femur in 2004 when one of us (A.B-M.) was reviewing the collection of nonhominin vertebrate
111 fossils temporarily stored at the University of Poitiers as part of a taphonomic survey of the late
112 Miocene assemblages from Toros-Menalla (Bergeret, 2004). We do not know the present
113 whereabouts of the TM 266 femur.

114 The ca. 250 mm-long specimen (Fig. 1) consists of a relatively well-preserved and robust left
115 femoral shaft. It lacks any gross morphological evidence that could confirm its maturity. In
116 addition to longitudinal cracks on the shaft, and some erosion at the distal end, there is evidence
117 of surface weathering and damage consistent with gnawing by a carnivore. As with other fossils
118 from this locality at Toros-Menalla, the TM 266 femur was partially covered by a crust of iron
119 and manganese oxides, beneath which the bone surface is roughened. The original shaft
120 morphology is well-preserved proximally, but the distal end is damaged and slightly compressed
121 anteroposteriorly. The proximal fracture surface preserves the base of the femoral neck,
122 including the distal part of the lesser trochanter (Fig. 2). Enough is preserved to indicate a range
123 of possible neck-shaft angles (Supplementary Online Material [SOM] Fig. S1), but we
124 emphasize that any firm statements about the angulation of the neck are not possible. We
125 estimate the distal break is close to what would have been the junction between the diaphysis and
126 the distal epiphysis: a reasonable estimate of the biomechanical length (Ruff, 2002) of the TM
127 266 femur is >280 mm (SOM Fig. S2).

128 Given that the fossil assemblage from Toros-Menalla includes both hyaenids (e.g.,
129 *Chasmaporthetes*, *Belbus*, *Hyaenictitherium* and *Werdelinus*) and felids (e.g., *Dinofelis*,
130 *Machairodus*, *Lokotunjailurus* and *Tchadailurus*; Vignaud et al., 2002; Bonis et al., 2005, 2007,
131 2010a, b; Peigné et al., 2005; Le Fur et al., 2014), we explored the possibility that the TM 266
132 femur belongs to a carnivoran. However, in carnivorans the neck-shaft angle is usually lower, the
133 proximal shaft is typically not anteroposteriorly flattened, and the intertrochanteric region has a
134 characteristically medially-directed crest that should have been apparent in what is preserved of
135 the lesser trochanter. The TM 266 femoral shaft is convex anteroposteriorly throughout its
136 length. Carnivoran femora are also bowed, but normally only in the distal part of the shaft (Pale

137 and Lambert, 1971; Werdelin and Lewis, 2001; Werdelin, 2003; France, 2011; see also
138 <https://www.archeozoo.org/archeozootheque/>). For these reasons, we consider it much more
139 likely that the TM 266 femoral shaft belongs to a primate than to a carnivoran. Given that the
140 only other fossil evidence for a large-bodied primate has been assigned to *S. tchadensis*, and that
141 the TM 266 cranium and the femur were found in the same location (Beauvilain and Watté,
142 2009: Fig. 1a), it is a reasonable working assumption that the TM 266 femur should also be
143 assigned to *S. tchadensis*.

144

145 **2. Materials and methods**

146

147 *2.1. Comparative materials*

148

149 The comparative data used in the analyses include measurements taken from the partial
150 femora BAR 1002'00 and BAR 1003'00, representing *O. tugenensis*, and from samples
151 representing australopiths (*Australopithecus* and *Paranthropus*), modern humans (*H. sapiens*)
152 and extant great apes (*Pan*, *Gorilla*, *Pongo*). Two late Miocene great apes, *Rudapithecus*
153 *hungaricus* and *Hispanopithecus laietanus*, were also included in the comparative analysis of the
154 cross-sectional shape of the distal femoral shaft (see below).

155 Measurements of the two *O. tugenensis* femora and the data used in the analysis of the shaft
156 curvature are based on CT-images whose technical characteristics are detailed in Galik et al.
157 (2004). Additional measurements of BAR 1002'00 and BAR 1003'00 were taken from Senut et
158 al. (2001), Pickford et al. (2002), Nakatsukasa et al. (2007), Puymerau (2011, 2017, and original
159 data).

160 The australopith sample, which includes representatives of *Australopithecus afarensis*,
161 *Australopithecus africanus*, *Australopithecus sediba*, *Paranthropus robustus* and presumed
162 *Paranthropus boisei*, consists of the following specimens: A.L. 128-1, A.L. 152-2, A.L. 333-131,
163 A.L. 333-142, A.L. 827-1 (Ward et al., 2012); A.L. 129-1 (Johanson and Coppens, 1976); A.L.
164 211-1 (Harmon, 2006); A.L. 288-1ap (Johanson et al., 1982; Haeusler and McHenry, 2004);
165 MAK-VP 1/1 (Lovejoy et al., 2002); StW 573 (Heaton et al., 2019); SK 82, SK 97, StW 99, and
166 U.W. 88-4,5,39 (MH1; measured by D.M. on the originals; Marchi et al., 2017); A.L. 333-3 and
167 KNM-ER 738 (measured by D.M. on a high-quality cast at the Evolutionary Studies Institute,
168 University of the Witwatersrand, Johannesburg, South Africa; Marchi et al., 2017). Data from
169 the X-ray microtomographic (μ XCT) record of the left femur of the A.L. 288-1ap *A. afarensis*
170 partial skeleton (Johanson et al., 1982; Ruff et al., 2016) was also included in the comparative
171 analysis of the distal cross-sectional shape (courtesy of C.B. Ruff and J.W. Kappelman).

172 Data for modern humans come from several sources. Ninety-six adult individuals of both
173 sexes are from the Bronze Age necropolis of Olmo di Nogara, northern Italy, stored at the
174 Department of Biology, University of Pisa (measured by D.M.). Data from μ XCT images
175 (generated at the South African Nuclear Energy Corporation SOC Ltd, Pelindaba, South Africa)
176 of 10 adult individuals (5 females/5 males) of African ($n = 4$) and European ($n = 6$) ancestry
177 from the Pretoria Bone Collection, Pretoria, South Africa, were used in the comparative analysis
178 of the shaft curvature and in the analysis of distal cross-sectional shape.

179 Common chimpanzee data include measurements from 42 adult individuals (22 females/20
180 males) from: the Cleveland Museum of Natural History, Cleveland, USA; the Harvard Museum
181 of Comparative Zoology, Harvard, USA; the Smithsonian Institution's National Museum of
182 Natural History, Washington, D.C., USA; and the Yale Peabody Museum of Natural History,

183 New Haven, USA (Marchi et al., 2017). Data from 22 adult individuals (12 females/8 males/2
184 unknown) from the Digital Morphology Museum, Kyoto University Primate Research Institute
185 (KUPRI), Japan, 17 individuals from the Izu Shaboten Zoo and the Kyoto City Zoo;
186 <http://dmm.pri.kyoto-u.ac.jp/dmm/WebGallery/index.html>), one individual from the
187 Evolutionary Studies Institute, University of the Witwatersrand, Johannesburg, South Africa,
188 scanned at the South African Nuclear Energy Corporation SOC Ltd, Pelindaba, South Africa),
189 and four individuals from the Smithsonian Institution's National Museum of Natural History,
190 Washington, D.C., USA (MorphoSource, <https://www.morphosource.org/>), were also used in the
191 analyses of the shaft curvature and distal cross-sectional shape.

192 Gorilla data come from 47 adult individuals (20 females/27 males) from the Cleveland
193 Museum of Natural History, Cleveland, USA; the Harvard Museum of Comparative Zoology,
194 Harvard, USA; the Smithsonian Institution's National Museum of Natural History, Washington,
195 D.C., USA; and the Yale Peabody Museum of Natural History, New Haven, USA (Marchi et al.,
196 2017). Data from the surface model/CT record of 20 adult individuals (9 females/11 males) from
197 the Digital Morphology Museum, Kyoto University Primate Research Institute (KUPRI), Japan,
198 four individuals from the Higashiyama Zoo, the Fukuoka City Zoo and the Kobe Oji Zoo;
199 <http://dmm.pri.kyoto-u.ac.jp/dmm/WebGallery/index.html>), ten individuals from the Powell-
200 Cotton Museum, Birchington-on-Sea, UK scanned at the Cambridge Biotomography Centre,
201 Department of Zoology, University of Cambridge, Cambridge, UK, and six individuals from the
202 Smithsonian Institution's National Museum of Natural History, Washington, D.C., USA;
203 MorphoSource, <https://www.morphosource.org/>) were also used in the analyses of the shaft
204 curvature and distal cross-sectional shape.

205 Orangutan surface model/CT data were taken from five adult (2 females/3 males) and 3
206 juvenile (1 female/2 males) individuals from the Digital Morphology Museum, Kyoto University
207 Primate Research Institute (KUPRI), Japan ([http://dmm.pri.kyoto-](http://dmm.pri.kyoto-u.ac.jp/dmm/WebGallery/index.html)
208 [u.ac.jp/dmm/WebGallery/index.html](http://dmm.pri.kyoto-u.ac.jp/dmm/WebGallery/index.html)), and from seven individuals from the Smithsonian
209 Institution's National Museum of Natural History, Washington, D.C., USA (MorphoSource,
210 <https://www.morphosource.org/>). Data used for the analysis of shaft curvature and distal cross-
211 sectional shape come from 10 femora belonging to six individuals (i.e., eight femora are from
212 both sides of four individuals).

213 In the comparative analysis of the cross-sectional shape of the distal femoral shaft, we also
214 integrated the μ XCT-based evidence from *Rudapithecus hungaricus*, from Hungary (Kordos and
215 Begun, 2001; Begun et al., 2012; Ward et al., 2019), and *Hispanopithecus laietanus*, from Spain
216 (Moyà-Solà and Köhler, 1996; Köhler et al., 2002; Almécija et al., 2013; Pina, 2016).
217 *Rudapithecus* is represented by the right femur RUD 184 (courtesy of D.R. Begun and R.
218 Martin), while *Hispanopithecus* by the left femur IPS18800.28 (courtesy of M. Pina and of the
219 Institut Català de Paleontologia Miquel Crusafont).

220

221 2.2. *Methods*

222

223 The neck-shaft angle (i.e., between the long axis of the preserved shaft and the axis through
224 the midpoint of the preserved base of the neck; cf. Köhler et al., 2002) was measured using
225 ImageJ (Schneider et al., 2012) on different images of TM 266 in posterior view. Comparative
226 values of the neck-shaft angle for *Pan*, *Gorilla* and *Pongo* are a combination of our original
227 (μ)XCT-based measurements and data from Pina (2016).

228 For the assessment of the biomechanical length of the TM 266 femur, the 80% cross-sectional
229 level was defined as ca. 1 cm below the distal edge of the lesser trochanter, and the section at
230 50% (midshaft) at the point of maximum anteroposterior flexion of the shaft in medial and lateral
231 views (Ruff et al., 1999; Ruff, 2000, 2002; Puymeraill et al., 2012). Accordingly, the 20% cross
232 section has been established at approximately 2 cm from the distal-most point of the preserved
233 shaft (SOM Fig. S2).

234 For assessing the degree of anteroposterior curvature of the femoral shaft, we performed
235 bidimensional geometric morphometric (2DGM) analyses on the sketch of TM 266 (SOM Fig.
236 S3) and on the similarly-oriented virtual rendering of BAR 1002'00 (*Orrorin*), and on four
237 (μ)XCT-based records representing *H. sapiens*, *Pan*, *Gorilla* and *Pongo*. The images were
238 imported in TpsUtil64 (Rohlf, 2005) to create a TPS file. Using the TpsDig2 software v. 2.31
239 (Rohlf, 2005), a total of 25 equidistant semilandmarks were digitized along the anterior outline
240 between the point projected from the middle of the lesser trochanter (a, estimated in TM 266)
241 and ca. 40% of the biomechanical length (b, estimated in both TM 266 and BAR 1002'00 and
242 measured in all other specimens). We then performed generalized Procrustes analyses and a
243 principal component analysis (PCA) and computed the between-group PCA analyses (bgPCA)
244 based on the Procrustes residuals and using the extant taxa as groups. TM 266 and BAR 1002'00
245 were projected a posteriori in the bgPCA. The analyses were performed using the package ade4
246 v. 1.7-6 (Dray and Dufour, 2007) for R v. 3.6.3 (R Development Core Team, 2020).

247 To assess the cross-sectional morphology of the TM 266 shaft at its naturally-broken distal
248 end (Fig. 2a), which is ca. 15% of the biomechanical length, we firstly extracted the cortical shell
249 by manual delimitation of the endosteal and periosteal contours (SOM Fig. S4a). However, given
250 some damage and the slight anteroposterior compression in the distal shaft, in order to perform a

251 2D GM-based analysis of the cross-sectional morphology similar to that of the degree of
252 anteroposterior curvature, we generated and projected a posteriori in the analysis two outlines of
253 the TM 266 shaft approximating its original contour in two ways (SOM Fig. S4b, c). For
254 comparison, we virtually extracted the contours at 15% and 20% of the biomechanical length of
255 the same (μ)XCT-based records of femora representing *H. sapiens*, *Pan*, *Gorilla* and *Pongo*. In
256 this bgPCA analysis we also introduced the section at ca. 20% of the biomechanical length of
257 A.L. 288-1ap (*A. afarensis*; SOM Fig. S5a), those at ca. 17% and ca. 20% of IPS18800.28
258 (*Hispanopithecus*; SOM Fig. S5b, c), and that at ca. 20% of RUD 184 (*Rudapithecus*; SOM Fig.
259 S5d). The contours of IPS18800.28 did not require any correction, but the contour of RUD 184
260 was partially reconstructed to compensate for lateral damage and anteroposterior deformation
261 (SOM Fig. S5d). A total of 80 equidistant semilandmarks were digitized around the outer outline
262 of each cross section used in the analysis.

263

264 **3. Results**

265

266 *3.1. Comparative analysis*

267

268 The size and morphology of the TM 266 femoral shaft are much more consistent with it
269 belonging to a fossil hominid than to a fossil monkey. In terms of size and shape, the external
270 morphology of the shaft is closer to that of the common chimpanzee than to modern humans,
271 gorillas or orangutans (Table 1). This is most evidently the case when we consider the
272 anteroposterior curvature and the cross-sectional morphology of the shaft. The results of the
273 bgPCA for the anteroposterior curvature (Fig. 3) locate TM 266 in the same shape space as *Pan*.

274 The analysis also tends to separate *Pongo*, mostly in the positive values of bgPC1, from the other
275 extant hominids, mostly in the negative values (or in the negative values close to the axis origin).
276 *Pongo* is distinguished by an outline which is slightly concave proximally and nearly flat
277 distally, whereas the other extant hominids show an outline that is flat proximally and more
278 convex distally. Along bgPC2, *Homo* and *Pongo* (mostly in the positive values) are partially
279 discriminated from *Gorilla* and *Pan* (mostly in the negative values) by a slightly convex, or even
280 nearly flat shape, distinct from the more sinusoidal outline of the African apes. TM 266 and BAR
281 1002'00 (*Orrorin*) are at different locations in this morphospace: TM 266 is within the variation
282 of *Pan*, near that of *Gorilla*, and outside the morphospace occupied by *Homo* and *Pongo*, while
283 BAR 1002'00 falls between *Homo* and *Pongo*, and away from the African ape morphospace (Fig.
284 3).

285 Likewise, the cross-sectional morphology of the TM 266 distal shaft (Fig. 2a) is most similar
286 to that of *Pan* (Fig. 4). Indeed, in the morphospace of the bgPCA (Fig. 5), the subovoidal cross-
287 sectional outlines of TM 266 and *Rudapithecus* are distinct from all of the extant hominids,
288 except *Pan*, while the more anteroposteriorly compressed outline of *Hispanopithecus* is separate
289 from modern humans, far from that of *Pan*, and closer to the morphology of *Pongo* and *Gorilla*.
290 In this context, it is noteworthy that the closest fit for the subrounded cross section of *A.*
291 *afarensis* are extant humans (Fig. 5).

292 The neck-shaft angle estimated from the preserved morphology (Fig. 2b) ranges between 138°
293 and 146° (SOM Fig. S1). If we use the conservative estimate of >135° provided in Table 1, the
294 angle in TM 266 is likely to have been higher than in BAR 1002'00, and above the range seen in
295 the extant African apes (Table 1). It was likely closer to the range of values for *Pongo* and
296 *Hispanopithecus* (Köhler et al., 2002; Pina, 2016).

297 The TM 266 femoral shaft is larger at all comparable cross-sectional levels than the average
298 for *Pan* (Table 1), but the reconstructed biomechanical length is similar to the estimates for *O.*
299 *tugenensis* (BAR 1002'00: 288 mm; BAR 1003'00: 297 mm; Nakatsukasa et al., 2007;
300 Puymerau, 2017 and original data). This suggests that the body mass of the TM 266 individual
301 likely exceeded the ca. 47 kg estimated for the body mass of BAR 1003'00, the larger of the two
302 better-preserved *O. tugenensis* femora (Grabowski et al., 2018; see also Nakatsukasa et al.,
303 2007).

304

305 3.2. *Functional assessment*

306

307 An erect posture and bipedal locomotion have traditionally been accepted as one of the
308 defining features of the hominin clade (e.g., Le Gros Clark, 1955), and they are routinely used as
309 criteria to assess whether Pliocene hominid fossils should be included in the hominin clade (e.g.,
310 Haile-Selassie et al., 2004; White et al., 2009; Simpson, 2013; Pilbeam and Lieberman, 2017).
311 That is not to say that all habitually bipedal hominids are necessarily hominins, but the consensus
312 is that to be a member of the hominin clade the morphology of a candidate species needs to be
313 consistent with habitual bipedalism. If it could be demonstrated that the morphology of the TM
314 266 femoral shaft was consistent with its owner being an habitual biped, this would strengthen
315 the case for it being a hominin.

316 There are at least two lines of evidence that can be pursued to investigate this. First, is the
317 morphology of TM 266 more similar to the only extant habitual biped, modern humans, than to
318 closely-related extant taxa that do not practise habitual bipedalism? Given the results of the
319 comparative analyses in the previous section, the overall morphology of TM 266 appears to be

320 closer to that of common chimpanzees than it is to habitually bipedal modern humans. In
321 addition, in bipedal hominins with medial angulation of the shaft associated with a valgus knee,
322 there is a reduction in shaft width as you move from the subtrochanteric to the midshaft level
323 (i.e., distally within the 80–50% portion of the estimated femoral biomechanical length; Ruff et
324 al., 2016). The TM 266 femoral shaft lacks this distal taper.

325 But we know the hominin clade includes taxa that are almost certainly habitual bipeds, yet
326 their femoral morphology differs from that of modern humans (Lovejoy and Heiple, 1972;
327 Richmond and Jungers, 2008). Unfortunately, the TM 266 femur lacks the regions—the
328 proximal and distal epiphyses—that are most informative about the functional role (sensu Bock
329 and von Wahlert, 1965) of the femur (e.g., Lovejoy, 1988; Richmond and Jungers, 2008; Ruff
330 and Higgins, 2013; Marchi et al., 2017; Cazenave et al., 2019; Pina et al., 2019; Sukhdeo et al.,
331 2020). Although the proximal epiphysis is missing in TM 266, the proximal end of BAR
332 1002'00, the most complete of the three partial femora attributed to *O. tugenensis* (Senut et al.,
333 2001; Pickford et al., 2002), is relatively complete and well preserved (Fig. 6). Its external and
334 internal morphology have been the subject of relatively intensive investigation, with most
335 authors concluding that BAR 1002'00 is consistent with australopith-like habitual bipedalism
336 (Pickford et al., 2002; Galik et al., 2004; Nakatsukasa et al., 2007; Richmond and Jungers, 2008,
337 2012; Kuperavage et al., 2018). Exceptions to this consensus are Almécija et al. (2013), who saw
338 differences between the bipedalism of BAR 1002'00 and australopiths, and Ohman et al. (2005),
339 who questioned the interpretation of the internal morphology. Bleuze (2012) conducted a
340 comparative study using the cross-sectional geometry of the proximal end of the femoral shaft,
341 and concluded that BAR 1002'00 and BAR 1003'00 resemble the australopiths. So, if the BAR
342 1002'00 femur belongs to an habitual biped, and if the parts of the femur that are preserved in

343 common in TM 266 and BAR 1002'00 resemble each other as closely as two members of the
344 same taxon, then this would be a second line of evidence in support of the hypothesis that *S.*
345 *tchadensis* is a habitual biped. The results of our preliminary analysis of anteroposterior
346 curvature suggest the opposite, in that the difference in anteroposterior curvature in multivariate
347 space between TM 266 and BAR 1002'00 exceeds the variation we see within any of the extant
348 great apes (Fig. 3).

349 The functional implications of the non-metrical morphology of the TM 266 femur are less
350 clear. There is no spiral line, nor is there a gluteal tuberosity. Intertrochanteric and spiral lines
351 are both evident in BAR 1002'00, and both BAR 1002'00 and BAR 1003'00 have a gluteal
352 tuberosity (Pickford et al., 2002). However, the evolutionary significance of the latter is unclear,
353 for while it is usually absent in extant African apes (Lovejoy et al., 2002), it is present in some
354 Miocene apes (Nakatsusaka and Kunitatsu, 2004; Almécija et al., 2013; Pilbeam and
355 Lieberman, 2017; Pina et al., 2019). The region that would provide evidence of an
356 intertrochanteric line is missing in TM 266. The presence of the pectineal line, which is marked
357 in *O. tugenensis*, could not be confidently assessed in TM 266 because of damage to the surface
358 bone in that area (Fig. 2b), but there is evidence of a modestly-developed lateral spiral pilaster, a
359 feature common in extant apes (Lovejoy et al., 2002), but absent in *O. tugenensis* (Pickford et al.,
360 2002).

361 Below the greater trochanter, the posterior surface of the TM 266 femur bears a laterally-
362 convex crest that extends distally to the midline where, proximal to the midshaft, it contributes to
363 a modest linea aspera. More distally the surface topography is poorly preserved (Fig. 2c). The
364 morphology of the posterior surface of the femoral shaft is unlike that seen in BAR 1002'00,

365 which has a salient and wide midline crest on the posterior aspect of the shaft (Senut et al., 2001;
366 Pickford et al., 2002).

367 Given the broader comparative context of the morphology of the TM 266 femur, there is no
368 compelling evidence that it belongs to a habitual biped, something that would strengthen the case
369 for *S. tchadensis* being a hominin. Indeed, the shape differences between TM 266 and BAR
370 1002'00 suggest that the locomotor modes of *S. tchadensis* and *O. tugenensis* were different.

371

372 **4. Discussion**

373

374 Guy et al. (2005: 18839) suggested that “further research is needed to determine the
375 evolutionary relationships between *Sahelanthropus* and known Miocene and Pliocene hominids”,
376 and in the final section of their paper they made a plea for “more information” (Guy et al., 2005:
377 18840). In relation to claims that evidence from the TM 266 cranium was consistent with *S.*
378 *tchadensis* being a habitual biped, Richmond and Jungers (2008: 1662) suggested that
379 “postcranial fossils are needed to confirm this conclusion”. We review below what can be said
380 about the taxonomy and functional morphology of the TM 266 femoral shaft in descending order
381 of confidence. It is unfortunate that the information provided by the TM 266 femur is limited to
382 the shaft. We would have greater confidence in our taxonomic and functional analysis if that
383 were not the case.

384 We are most confident that the TM 266 femoral shaft belongs to a hominid sensu lato. It
385 could sample a hominid hitherto unrepresented at Toros-Menalla, but a more parsimonious
386 working hypothesis is that it belongs to *S. tchadensis*. The differences between TM 266 and the
387 *O. tugenensis* partial femur BAR 1002'00 are substantial, and are consistent with maintaining at

388 least a species-level distinction between *S. tchadensis* and *O. tugenensis*, but most of what has
389 been published about the femoral morphology of *O. tugenensis* is based on the analysis of just
390 one, BAR 1002'00, of three femoral specimens assigned to that taxon. Finally, if the TM 266
391 femoral shaft belongs to *S. tchadensis*, we cannot be confident that the latter was a habitual
392 biped.

393 We must emphasize that our observations on the TM 266 femoral shaft are preliminary. They
394 are limited to what we can glean from the literature, plus limited and brief access to the original
395 fossil. We hope that those with curatorial responsibility for the original specimen will conduct a
396 more detailed and thorough comparative study, including assessments of cross-sectional
397 geometric properties and internal structure.

398 However, on the assumption that the TM 266 femur is a justified addition to the hypodigm of
399 *S. tchadensis*, what are the implications of our preliminary assessment of the new evidence for
400 the evolutionary relationships of *S. tchadensis*? Does the new evidence have any broader
401 implications for our understanding of hominid and hominin evolution in Africa at this time (i.e.,
402 ca. 7–6 Ma)?

403 There are an impressive number of differences between the morphology of
404 chimpanzees/bonobos and modern humans, but the differences between the late Miocene
405 ancestors of modern humans and chimpanzees/bonobos are likely to have been much more
406 subtle. Some of the features that distinguish modern humans from chimpanzees/bonobos, such as
407 those linked with bipedalism, can be traced back a long way (Almécija et al., 2013; Böhme et al.,
408 2019). Others, such as the relatively diminutive jaws and chewing teeth of modern humans, were
409 acquired more recently and thus cannot be used to tell the difference between stem hominins and
410 stem panins.

411 Given these caveats, how do we go about telling a stem hominin from a stem panin? The
412 conventional assumption is that a stem panin would have had a projecting face accommodating
413 an elongated jaw bearing relatively small chewing teeth and relatively and absolutely large,
414 sexually-dimorphic, honed canine teeth, and a locomotor system adapted for arboreal
415 quadrupedalism (Pilbeam and Lieberman, 2017). A stem hominin, on the other hand, would have
416 been distinguished by cranial and other skeletal adaptations to a predominantly upright posture
417 and skeletal and other adaptations for a locomotor strategy that includes substantial bouts of
418 terrestrial bipedalism. These features would be combined with a masticatory apparatus that
419 combines relatively large chewing teeth and modest-sized canines. These inferences are working
420 hypotheses that will need to be reviewed and tested as the relevant evidence is uncovered (Guy et
421 al., 2005).

422 It should be clear from the foregoing that the presence of only one, or even a few, of the
423 features that possibly distinguish early hominins from early panins, may not be sufficient to
424 identify a fossil as a hominin or a panin. This is because there is evidence that primates, like
425 many other groups of mammals, are affected by homoplasy (aka false homology; Diogo and
426 Wood, 2011). Phenotypic homoplasies are morphological features that are shared by two, or
427 more, taxa that are not seen in the most recent common ancestor of those taxa. The possibility of
428 convergent and/or parallel evolution—both of which can result in homoplasy—means that it is
429 not impossible, indeed it may even be probable, that some of what many have come to regard as
430 key morphological adaptations at the base of the hominin lineage may have arisen more than
431 once. If that is the case, then what characterizes hominins (and panins and the other great ape
432 lineages) may not be particular items of morphology, single characters, but particular
433 combinations of characters.

434 It is possible that *S. tchadensis* is a stem hominin with some reduction of the canine and loss
435 of the honing complex, but without the femoral adaptations to terrestrial bipedalism that are seen
436 in *A. afarensis* and *O. tugenensis* (Pickford et al., 2002; Galik et al., 2004; Richmond and
437 Jungers, 2008; Almécija et al., 2013). It has been suggested that the early Pliocene *Ardipithecus*
438 *ramidus* (Lovejoy et al., 2009; White et al., 2009; Simpson et al., 2019) was an orthograde biped,
439 but it is difficult to see how its abducted hallux is compatible with terrestrial bipedality. Based on
440 our analyses, the TM 266 partial femur lacks any feature consistent with regular bouts of
441 terrestrial bipedal travel; instead, its gross morphology suggests a derived *Pan*-like bauplan.
442 Thus, if there is compelling evidence that *S. tchadensis* is a stem hominin, then bipedalism can
443 no longer be seen as a requirement for inclusion in the hominin clade.

444 But, being a stem hominin or a stem panin, or their most recent common ancestor, may not be
445 the only options for *S. tchadensis*. Given what we have learned about the evolutionary history of
446 the clade that includes the extant great apes, it is likely, and indeed probable, that during the late
447 Miocene and the early Pliocene there was a modest adaptive radiation of African hominids that
448 includes taxa that are neither hominins or panins as defined above (Wood and Harrison, 2011).
449 Any such extinct groups are likely to include taxa with novel morphology, or with novel
450 combinations of morphology we also see in hominins or panins. Given the mix of inferred
451 primitive and inferred derived features in *S. tchadensis*, we suggest it could belong to a group
452 that has no living representative.

453

454 **5. Conclusion**

455

456 The lack of clear evidence that the TM 266 femur is from a hominid that was habitually
457 bipedal further weakens the already weak case (Mongle et al., 2019) for *S. tchadensis* being a
458 stem hominin. However, this in no way diminishes the significance of *S. tchadensis* (Brunet et
459 al., 2002). There is a compelling evidence that, for at least the last four million years, the
460 hominin clade shows evidence of taxonomic, and thus lineage, diversity (Haile-Selassie et al.,
461 2016; Wood and Boyle, 2016). If this is the case, the minority of the extinct hominin taxa that
462 have been recognized are likely to be the ancestors of modern humans; most will turn out to be
463 non-ancestral close relatives, but presently it is difficult to sort ancestors from non-ancestral
464 close relatives. There is no logical reason to think that the same problems and limitations do not
465 also apply to late Miocene hominids. It will not be easy, especially if the fossil evidence is
466 relatively meager, to work out which late Miocene taxa are hominins, which are panins, and
467 which are neither. As one of us has suggested, "exactly where in Africa, and under what
468 circumstances, the ape-human demarcation began, and when, how and why the ape-human
469 boundary became irrevocably established, are important research challenges that are still
470 unresolved" (Wood, 2017: 103). But if we treat the hominin status of *S. tchadensis*, or any other
471 enigmatic taxon, as a given and not a hypothesis, we run the risk of adding further confusion to a
472 picture that is already "complicated and less easy to resolve" (Guy, et al., 2005: 18839).

473

474 **References**

475

476 Ahern, J.C., 2005. Foramen magnum position variation in *Pan troglodytes*, Plio-Pleistocene
477 hominids, and recent *Homo sapiens*: Implications for recognizing the earliest hominids.
478 American Journal of Physical Anthropology 127, 267-276.

479 Almécija, S., Tallman, M., Alba, D.M., Pina, M., Moyà-Solà, S. Jungers, W.L., 2013. The femur
480 of *Orrorin tugenensis* exhibits morphometric affinities with both Miocene apes and later
481 hominins. *Nature Communications* 4, 2888.

482 Beauvilain, A., Watté, J.-P., 2009. Was Toumaï (*Sahelanthropus tchadensis*) buried?
483 *Anthropologie* 47, 1-6.

484 Begun, D.R., Nargolwalla, M.C., Kordos, L., 2012. European Miocene hominids and the origin
485 of the African ape and human clade. *Evolutionary Anthropology* 21, 10-23.

486 Bergeret, A., 2004. Approche taphonomique d'un assemblage miocène de vertébrés fossiles du
487 désert du Djourab (Tchad): implications paléoécologiques. DEA Thesis, Université de
488 Poitiers.

489 Bleuze, M., 2012. Proximal femoral diaphyseal cross-sectional geometry in *Orrorin tugenensis*.
490 *Journal of Comparative Human Biology*, 63, 153-166.

491 Bock, W., von Wahlert, G., 1965. Adaptation and the form-function complex. *Evolution* 19, 269-
492 299.

493 Böhme, M., Spassov, N., Fuss, J., Tröscher, A., Deane, A.S., Prieto, J., Kirscher, U., Lechner, T.,
494 Begun, D.R., 2019. A new Miocene ape and locomotion in the ancestor of great apes and
495 humans. *Nature* 575, 489-493.

496 Bonis, L. de, Peigné, S., Guy, F., Likius, A., Mackaye, H.T., Vignaud, P., Brunet, M., 2010a.
497 *Hyaenidae* (Carnivora) from the late Miocene of Toros-Menalla, Chad. *Journal of African*
498 *Earth Sciences* 58, 561-679.

499 Bonis, L. de, Peigné, S., Likius, A., Mackaye, H.T., Vignaud, P., Brunet, M., 2005.
500 *Hyaenictitherium minimum*, a new ictithere (Mammalia, Carnivora, *Hyaenidae*) from the Late
501 Miocene of Toros-Menalla, Chad. *Comptes Rendus Palevol* 4, 671-679.

502 Bonis, L. de, Peigné, S., Likius, A., Mackaye, H.T., Vignaud, P., Brunet, M., 2007. First
503 occurrence of the "hunting hyena" *Chasmaporthetes* in the Late Miocene fossil bearing
504 localities of Toros Menalla Chad (Africa). Bulletin de la Société Géologique de France 178,
505 317-326.

506 Bonis, L. de, Peigné, S., Likius, A., Mackaye, H.T., Vignaud, P., Brunet, M., 2010b. New sabre-
507 toothed cats in the late Miocene of Toros Menalla (Chad). Comptes Rendus Palevol 9, 221-
508 227.

509 Bradley, B., 2008. Reconstructing phylogenies and phenotypes: A molecular view of human
510 evolution. Journal of Anatomy 212, 337-353.

511 Brunet, M., Guy, F., Boisserie, J.-R., Djimdoumalbaye, A., Lehmann, T., Lihoreau, F., Louchart,
512 A., Schuster, M., Tafforeau, P., Likius, A., Mackaye, H.T., Blondel, C., Bocherens, H., de
513 Bonis, L., Coppens, Y., Denis, C., Douring, P. Eisenmann, V., Flisch, A., Geraads, D.,
514 Lopez-Martinez, N., Otero, O., Peláez-Campomanes, P., Pilbeam, D., Ponce de León, M.S.,
515 Vignaud, P., Viriot, L., Zollikofer, C., 2004. "Toumaï", Miocène supérieur du Tchad, le
516 nouveau doyen du rameau humain. Comptes Rendus Palevol 3, 277-285.

517 Brunet, M., Guy, F., Pilbeam, D., Lieberman, D.E., Likius, A., Mackaye, H.T., Ponce de León,
518 M.S., Zollikofer, C., Vignaud, P., 2005. New material of the earliest hominid from the Upper
519 Miocene of Chad. Nature 434,752-755.

520 Brunet, M., Guy, F., Pilbeam, D., Mackaye, H.T., Likius, A., Ahounta, D., Beauvilain, A.,
521 Blondel, C., Bocherens, H., Boisserie, J.-R., de Bonis, L., Coppens, Y., Dejax, J., Denys, C.,
522 Douring, P., Eisenmann, V., Gongdibe, F., Fronty, P., Geraads, D., Lehmann, T., Lihoreau,
523 F., Louchart, A., Mahamat, A., Merceron, G., Mouchelin, G., Otero, O., Peláez -
524 Campomanes, P., Ponce de León, M.S., Rage, J.-C., Sapanet, M., Schuster, M., Sudre, J.,

525 Tassy, P., Valentin, X., Vignaud, P., Viriot, L., Zazzo, A., Zollikofer, C., 2002. A new
526 hominid from the Upper Miocene of Chad, Central Africa. *Nature* 418,145-151.

527 Brunet, M., Jaeger, J.-J., 2017. De l'origine des anthropoïdes à l'émergence de la famille
528 humaine. *Comptes Rendus Palevol* 16, 189-195.

529 Cazenave, M., Braga, J., Oettlé, A., Pickering, T.R., Heaton, J.L., Nakatsukasa, M., Thackeray
530 J.F., de Beer, F., Hoffman, J., Dumoncel, J., Macchiarelli, R., 2019. Cortical bone distribution
531 in the femoral neck of *Paranthropus robustus*. *Journal of Human Evolution* 135, 102666.

532 Diogo, R., Molnar, J.L., Wood, B., 2017. Bonobo anatomy reveals stasis and mosaicism in
533 chimpanzee evolution, and supports bonobos as the most appropriate extant model for the
534 common ancestor of chimpanzees and humans. *Scientific Reports* 7, 608.

535 Diogo, R., Wood, B., 2011. Soft-tissue anatomy of the primates: phylogenetic analyses based on
536 the muscles of the head, neck, pectoral region and upper limb, with notes on the evolution of
537 these muscles. *Journal of Anatomy* 219, 273–359.

538 Dray, S., Dufour, A.B., 2007. The ade4 package: Implementing the duality diagram for
539 ecologists. *Journal of Statistical Software* 22, 1-20.

540 Emonet, E.-G., Andossa, L., Mackaye, H.T., Brunet, M., 2014. Subocclusal dental morphology
541 of *Sahelanthropus tchadensis* and the evolution of teeth in hominins. *American Journal of*
542 *Physical Anthropology* 153, 116-123.

543 France, D.L., 2011. *Human and Nonhuman Bone Identification. A Concise Field Guide*. CRC
544 Press, Boca Raton.

545 Galik, K., Senut, B., Pickford, M., Gommery, D., Treil, J., Kuperavage, A.J., Eckhardt, R.B.,
546 2004. External and internal morphology of the BAR 1002000 *Orrorin tugenensis* femur.
547 *Science* 305, 1450-1453.

548 Grabowski, M., Hatala, K.G., Jungers, W.L., 2018. Body mass estimates of the earliest possible
549 hominins and implications for the last common ancestor. *Journal of Human Evolution* 122,
550 84-92.

551 Guy, F., Lieberman, D.E., Pilbeam, D., Ponce de León, M., Likius, A., Mackaye, H.T., Vignaud,
552 P., Zollikofer, C., Brunet, M., 2005. Morphological affinities of the *Sahelanthropus*
553 *tchadensis* (Late Miocene hominid from Chad) cranium. *Proceedings of the National*
554 *Academy of Sciences USA* 102, 18836-18841.

555 Haeusler, M., McHenry, H.M., 2004. Body proportions of *Homo habilis* reviewed. *Journal of*
556 *Human Evolution* 46, 433-465.

557 Haile-Selassie, Y., Melillo, S.M., Su, D.F., 2016. The Pliocene hominin diversity conundrum:
558 Do more fossils mean less clarity? *Proceedings of the National Academy of Sciences USA*
559 113, 6364-6371.

560 Haile-Selassie, Y., Suwa, G., White, T.D., 2004. Late Miocene teeth from Middle Awash,
561 Ethiopia, and early hominid dental evolution. *Science* 303, 1503-1505.

562 Harmon, E.H., 2006. Size and shape variation in *Australopithecus afarensis* proximal femora.
563 *Journal of Human Evolution* 51, 217-227.

564 Heaton, J.L., Pickering, T.R., Carlson, K.J., Crompton, R.H., Jashashvili, T., Beaudet, A.,
565 Bruxelles, L., Kuman, K., Heile, A.J., Stratford, D., Clarke, R.J., 2019. The long limb bones
566 of the StW 573 *Australopithecus* skeleton from Sterkfontein Member 2: Descriptions and
567 proportions. *Journal of Human Evolution* 133, 167-197.

568 Johanson, D.C., Coppens, Y., 1976. A preliminary anatomical diagnosis of the first
569 Plio/Pleistocene hominid discoveries in the Central Afar, Ethiopia. *American Journal of*
570 *Physical Anthropology* 45, 217-234.

571 Johanson, D.C., Lovejoy, C.O., Kimbel W.H., White, T.D., Ward, S.C., Bush, M.E., Latimer,
572 B.M., Coppens, Y., 1982. Morphology of the Pliocene partial hominid skeleton (A.L. 288-1)
573 from the Hadar formation, Ethiopia. *American Journal of Physical Anthropology* 57, 403-451.

574 Köhler, M., Alba, D.M., Moyà, S., MacLatchy, L., 2002. Taxonomic affinities of the Eppelsheim
575 femur. *American Journal of Physical Anthropology* 119, 297-304.

576 Kordos, L., Begun, D.R., 2001. Primates from Rudabánya: Allocation of specimens to
577 individuals, sex and age categories. *Journal of Human Evolution* 40, 17-39.

578 Kuperavage, A., Pokrajac, D., Chavanaves, S., Eckhardt, R.B., 2018. Earliest known hominin
579 calcar femorale in *Orrorin tugenensis* provides further internal anatomical evidence for origin
580 of human bipedal locomotion. *The Anatomical Record* 30, 1834-1839.

581 Langergraber, K.E., Prüfer, K., Rowney, C., Boesch, C., Crockford, C., Fawcett, K., Inoue, E.,
582 Inoue-Muruyama, M., Mitani, J.C., Muller, M.N., Robbins, M.M., Schubert, G., Stoinski,
583 T.S., Viola, B., Watts, D., Wittig, R.M., Wrangham, R.W., Zuberbühler, Pääbo, S., Vigilant,
584 L., 2012. Generation times in wild chimpanzees and gorillas suggest earlier divergence times
585 in great ape and human evolution. *Proceedings of the National Academy of Sciences USA*
586 109, 15716-15721.

587 Lebatard A.-E., Bourlès, D.L., Durringer, P., Jolivet, M., Braucher, R., Carcaillet, J., Schuster,
588 M., Arnaud, N., Monié, P., Lihoreau, F., Likius, A., Mackaye, H.T., Vignaud, P., Brunet, M.,
589 2008. Cosmogenic nuclide dating of *Sahelanthropus tchadensis* and *Australopithecus*
590 *bahrelghazali*: Mio-Pliocene hominids from Chad. *Proceedings of the National Academy of*
591 *Sciences USA* 105, 3226-3231.

592 Le Fur, S., Fara, E., Mackaye, H.T., Vignaud, P., Brunet, M., 2014. Toros-Menalla (Chad, 7
593 Ma), the earliest hominin-bearing area: How many mammal paleocommunities? *Journal of*
594 *Human Evolution* 69, 79-90.

595 Le Gros Clark, W.E., 1955. *The Fossil Evidence for Human Evolution: An Introduction to the*
596 *Study of Paleoanthropology*. University of Chicago Press, Chicago, IL.

597 Lovejoy, C.O., 1988. Evolution of Human Walking. *Scientific American* 259(5), 118-125.

598 Lovejoy, C.O., Heiple, K.G., 1972. Proximal femoral anatomy of *Australopithecus*. *Nature* 235,
599 175-176.

600 Lovejoy, C.O., Meindl, R.S., Ohman, J.C., Heiple, K.G., White, T.D., 2002. The Maka femur
601 and its bearing on the antiquity of human walking: Applying contemporary concepts of
602 morphogenesis to the human fossil record. *American Journal of Physical Anthropology* 119,
603 97-133.

604 Lovejoy, C.O., Suwa, G., Simpson, S.W., Matternes, J.H., White, T.D., 2009. The great divides:
605 *Ardipithecus ramidus* reveals the postcrania of our last common ancestors with African apes.
606 *Science* 326, 101-106.

607 Marchi, D., Walker, C.S., Wei, P., Holliday, T.W., Churchill, S.E., Berger, L.R., DeSilva, J.M.,
608 2017. The thigh and leg of *Homo naledi*. *Journal of Human Evolution* 104, 174-204.

609 Mongle, C.S., Strait, D.S., Grine, F.E., 2019. Expanded character sampling underscores
610 phylogenetic stability of *Ardipithecus ramidus* as a basal hominin. *Journal of Human*
611 *Evolution* 131, 28-39.

612 Moorjani, P., Sankararaman, S., Fu, Q., Przeworski, M., Patterson, N., Reich, D., 2016. A
613 genetic method for dating ancient genomes provides a direct estimate of human generation

614 interval in the last 45,000 years. Proceedings of the National Academy of Sciences USA 113,
615 5652-5657.

616 Moyà-Solà, S., Köhler, M., 1996. A *Dryopithecus* skeleton and the origin of great-ape
617 locomotion. Nature 379, 156-159.

618 Nakatsusaka, M., Kunimatsu, Y., 2004. *Nacholapithecus* and its importance for understanding
619 hominoid evolution. Evolutionary Anthropology 18, 103-119.

620 Nakatsukasa, M., Pickford, M., Egi, N., Senut, B., 2007. Femur length, body mass, and stature
621 estimates of *Orrorin tugenensis*, a 6 Ma hominid from Kenya. Primates 48, 171-178.

622 Ohman, J.C., Lovejoy, C.O., White, T.D., 2005. Questions about *Orrorin* femur. Science 307,
623 845.

624 Pale, L., Lambert, C., 1971. Atlas Ostéologique pour Server à l'Identification des Mammifères
625 du Quaternaire. I. Les Membres. Carnivores. Editions CNRS, Paris.

626 Peigné, S., Bonis, L. de, Likius, A., Mackaye, H.T., Vignaud, P., Brunet, M., 2005. New
627 machairodontine (Carnivora, Felidae) from the Late Miocene hominid of Toros-Menalla
628 Chad. Comptes Rendus Palevol 4, 243-253.

629 Pickford, M., Senut, B., Gommery, D., Treil, J., 2002. Bipedalism in *Orrorin tugenensis* revealed
630 by its femora. Comptes Rendus Palevol 1, 1-13.

631 Pilbeam, D.R., Lieberman, D.E., 2017. Reconstructing the last common ancestor of chimpanzees
632 and humans. In: Muller, M.N., Wrangham, R.W., Pilbeam, D.R. (Eds), Chimpanzees and
633 Human Evolution. Belknap Press of Harvard University Press, Cambridge, MA., pp. 22-141.

634 Pina, M., 2016. Unraveling the positional behaviour of fossil hominoids: Morphofunctional and
635 structural analysis of the primate hindlimb. Ph.D. Dissertation, Universitat Autònoma de
636 Barcelona.

637 Pina, M., Alba, D.M., Moyà-Solà, S., Almécija, S., 2019. Femoral neck cortical bone distribution
638 of dryopithecine apes and the evolution of hominid locomotion. *Journal of Human Evolution*
639 136, 102651.

640 Prado-Martinez, J., Sudmant, P.H., Kidd, J.M., Li, H., Kelley, J.L., Lorente-Galdos, B.,
641 Veeramah, K.R., Woerner, A.E., O'Connor, T.D., Santpere, G., Cagan, A., Theunert, C.,
642 Casals, F., Laayouni, H., Munch, K., Hobolth, A., Halager, A.E., Malig, M., Hernandez-
643 Rodriguez, J., Hernando-Herraez, I., Prüfer, K., Pybus M., Johnstone, L., Lachmann M.,
644 Alkan, C., Twigg, D., Petit, N., Baker, C., Hormozdiari, F., Fernandez-Callejo, M., Dabad,
645 M., Wilson, M.L., Stevison, L., Camprubí, C., Carvalho, T., Ruiz-Herrera, A., Vives, L.,
646 Mele, M., Abello, T., Kondova, I., Bontrop, R.E., Pusey, A., Lankester, F., Kiyang, J.A.,
647 Bergl, R.A., Lonsdorf, E., Myers, S., Ventura, M., Gagneux, P., Comas, D., Siegmund, H.,
648 Blanc, J., Agueda-Calpena, L., Gut, M., Fulton, L., Tishkoff, S.A., Mullikin, J.C., Wilson,
649 R.K., Gut, I.G., Gonder, M.K., Ryder, O.A., Hahn, B.H., Navarro, A., Akey, J.M.,
650 Bertranpetit, J., Reich, D., Mailund, T., Schierup, M.H., Hvilsom, C., Andrés, A.M., Wall,
651 J.D., Bustamante, C.D., Hammer, M.F., Eichler, E.E., Marques-Bonet, T., 2013. Great ape
652 genetic diversity and population history. *Nature* 499, 471-475.

653 Puyménil, L., 2011. Caractérisation de l'endostructure et des propriétés biomécaniques de la
654 diaphyse fémorale: la signature de la bipédie et la reconstruction des paléo-répertoires
655 posturaux et locomoteurs des Hominines. Ph.D. Dissertation, Muséum national d'Histoire
656 naturelle, Paris.

657 Puyménil, L., 2017. The structural and mechanical properties of the *Orrorin tugenensis* femoral
658 shaft and the assessment of bipedalism in early hominins. In: Macchiarelli, R., Zanolli, C.

659 (Eds), Hominin Biomechanics, Virtual Anatomy and Inner Structural Morphology: From
660 Head to Toe. A Tribute to Laurent Puymeraul. *Comptes Rendus Palevol* 16, 493-498.

661 Puymeraul, L., Ruff, C.B., Bondioli, L., Widiyanto, H., Trinkaus, E., Macchiarelli, R., 2012.
662 Structural analysis of the Kresna 11 *Homo erectus* femoral shaft (Sangiran, Java). *Journal of*
663 *Human Evolution* 63, 741-749.

664 R Development Core Team, 2020 R: A language and environment for statistical computing. R
665 Foundation for Statistical Computing, Vienna.

666 Richmond, B.G., Jungers, W.L., 2008. *Orrorin tugenensis* femoral morphology and the evolution
667 of hominin bipedalism. *Science* 319, 1662-1665.

668 Richmond, B.G., Jungers, W.L., 2012. Hominin proximal femur morphology from the Tugen
669 Hills to Flores. In: Reynolds, S.C., Gallagher, A. (Eds), *African Genesis: Perspectives on*
670 *Hominin Evolution*. Cambridge University Press, Cambridge, pp. 248-267.

671 Rohlf, F.J., 2005. *TpsDig2*. *TpsSeries*. Department of Ecology and Evolution, SUNY, Stony
672 Brook, New York.

673 Ruff, C.B., 2000. Body size, body shape, and long bone strength in modern humans. *Journal of*
674 *Human Evolution* 38, 269-290.

675 Ruff, C.B., 2002. Long bone articular and diaphyseal structure in Old World monkeys and apes.
676 I: Locomotor effects. *American Journal of Physical Anthropology* 119, 305-342.

677 Ruff, C.B., Burgess, M.L., Ketcham, R.A., Kappelman, J., 2016. Limb bone structural
678 proportions and locomotor behavior in A.L. 288-1 ("Lucy"). *PLoS One* 11, e0166095.

679 Ruff, C.B., Higgins, R., 2013. Femoral neck structure and function in early hominins. *American*
680 *Journal of Physical Anthropology* 150, 512-525.

681 Ruff, C.B., McHenry, H.M., Thackeray, J.F., 1999. Cross-sectional morphology of the SK 82
682 and 97 proximal femora. *American Journal of Physical Anthropology* 109, 509-521.

683 Ruvolo, M., 1997. Molecular phylogeny of the hominoids: Inferences from multiple independent
684 DNA sequence data sets. *Molecular Biology and Evolution* 14, 248-65.

685 Schneider, C.A., Rasband, W.S., Eliceiri, K.W., 2012. NIH Image to ImageJ: 25 years of image
686 analysis. *Nature Methods* 9, 671-675.

687 Senut, B., Pickford, M., Gommery, D., Mein, P., Cheboi, K., Coppens, Y., 2001. First hominid
688 from the Miocene (Lukeino Formation, Kenya). *Comptes Rendus de l'Académie des Sciences*
689 *de Paris* 332, 137-144.

690 Simpson, S.W., 2013. Before *Australopithecus*: The earliest hominins. In: Begun, D.R. (Ed.), *A*
691 *Companion to Paleoanthropology*. Wiley-Blackwell, Malden, pp. 417-433.

692 Simpson, S.W., Levin, N.E., Quade, J., Rogers, M.J., Semaw, S., 2019. *Ardipithecus ramidus*
693 postcrania from the Gona Project area, Afar Regional State, Ethiopia. *Journal of Human*
694 *Evolution* 129, 1-45.

695 Smith, R.J., 2005. Species recognition in paleoanthropology; implications of small sample sizes.
696 In: Lieberman, D.E., Smith, R.J., Kelley, J. (Eds), *Interpreting the Past: Essays on Human,*
697 *Primate, and Mammal Evolution in Honor of David Pilbeam*. Brill Academic Publishers,
698 Boston, pp. 207-219.

699 Stone, A.C., Battistuzzi, F.U., Kubatko, L.S., Perry Jnr, G.H., Trudeau, E., Lin, H., Kumar, S.,
700 2010. More reliable estimates of divergence times in *Pan* using complete mt DNA sequences
701 and accounting for population structure. *Philosophical Transactions of the Royal Society B*
702 365, 3277-3288.

703 Strait, D.S., Grine, F.E., 2004. Inferring hominoid and early hominid phylogeny using
704 craniodental characters: the role of fossil taxa. *Journal of Human Evolution* 47, 399-452.

705 Sukhdeo, S., Parsons, J., Niu, X.M., Ryan, T.M., 2020. Trabecular bone structure in the distal
706 femur of humans, apes, and baboons. *The Anatomical Record* 303, 129-149.

707 Vignaud, P., Douring, P., Mackaye, H.T., Likius, A., Blondel, C., Boisserie, J.-R., de Bonis, L.,
708 Eisenmann, V., Etienne, M.-E., Geraads, D., Guy, F., Lehmann, T., Lihoreau, F., Lopez-
709 Martinez, N., Mourer-Chauviré, C., Otero, O., Rage, J.-C., Schuster, M., Viriot, L., Zazzo, A.,
710 Brunet, M., 2002. Geology and paleontology of the Upper Miocene Toros-Menalla hominid
711 locality, Chad. *Nature* 418, 152-155.

712 Ward, C.V., Hammond, A.S., Plavcan, J.M., Begun, D.R., 2019. A late Miocene hominid partial
713 pelvis from Hungary. *Journal of Human Evolution* 136, 102645.

714 Ward, C.V., Kimbel, W.H., Harmon, E.H., Johanson, D.C., 2012. New postcranial fossils of
715 *Australopithecus afarensis* from Hadar, Ethiopia (1990-2007). *Journal of Human Evolution*
716 63, 1-51.

717 Werdelin, L., 2003. Mio-Pliocene Carnivora from Lothagam, Kenya. In: Leakey, M.G., Harris,
718 J.M. (Eds), Lothagam. The Dawn of Humanity in Eastern Africa. Columbia University Press,
719 New York. 261-328.

720 Werdelin, L., Lewis, M.E., 2001. A revision of the genus *Dinofelis* (Mammalia, Felidae).
721 *Zoological Journal of the Linnean Society* 132, 147-258.

722 White, T.D., Asfaw, B., Beyene, Y., Haile-Selassie, Y., Lovejoy, C.O., Suwa, G., WoldeGabriel,
723 G., 2009. *Ardipithecus ramidus* and the paleobiology of early hominids. *Science* 326, 75-85.

724 Wolpoff, M.H., Hawks, J., Senut, B., Pickford M., Ahern J., 2006. An ape or *the* ape: Is the
725 Toumaï cranium TM 266 a hominid? *PaleoAnthropology* 2006, 36-50.

726 Wolpoff, M.H., Senut, B., Hawks, J., 2002. *Sahelanthropus* or '*Sahelpithecus*'? Nature 419, 581-
727 582.

728 Wood, B., 2017. Chalk and cheese 2.0. Journal of Human Evolution 113, 103-106.

729 Wood, B., Boyle, E.K., 2016. Hominin taxic diversity: Fact or fantasy? Yearbook of Physical
730 Anthropology 159, 37-78.

731 Wood, B., Harrison, T., 2011. The evolutionary context of the first hominins. Nature 470, 347-
732 352.

733 Zollikofer, C.P.E., Ponce de León, M.S., Lieberman, D.E., Guy, F., Pilbeam, D., Likius, A.,
734 Mackaye, H.T., Vignaud, P., Brunet, M., 2005. Virtual cranial reconstruction of
735 *Sahelanthropus tchadensis*. Nature 434,755-759.

736

737 **Caption to figures**

738

739 **Figure 1.** The partial femur TM 266-01-063 from Toros-Menalla, Chad, in anterior (a), posterior
740 (b), medial (c), and lateral (d) views. Scale bar = 2 cm.

741

742 **Figure 2.** Details of TM 266-01-063. a) The naturally-broken, sediment-filled and slightly
743 anteroposteriorly compressed distal end seen from below (anterior surface to the bottom; medial
744 surface to the right). b) Posterior view of the proximal end (medial surface to the right). c)
745 Posterolateral view of the midshaft region (medial surface to the right). Scale bar = 2 cm.

746

747 **Figure 3.** Between-group principal component analysis (bgPCA) of the Procrustes shape
748 coordinates of the anterior femoral shaft curvature in TM 266-01-063, BAR 1002'00 (*Orrorin*)
749 and four (μ)XCT-based subsamples representing *Homo sapiens* (*Homo* in the pink space), *Pan*,
750 *Gorilla* and *Pongo*.

751

752 **Figure 4.** Virtual extraction of the cortical shell by manual delimitation of the endosteal and
753 periosteal contours of the naturally broken and slightly anteroposteriorly compressed distal
754 section of TM 266-01-63 (cf. Fig. 2a) and of (μ)CT-based virtual cross sections extracted at 15%
755 (upper) and 20% (lower) of the biomechanical length in a female (F) and a male (M) femur
756 representing *Homo sapiens*, *Pan*, *Gorilla* and *Pongo*. Scale bar = 2 cm.

757

758 **Figure 5.** Between-group principal component analysis (bgPCA) of the Procrustes shape
759 coordinates of the cross-sectional contour of the distal femoral shaft in TM 266-01-063 (ca. 15%

760 of the estimated biomechanical length), A.L. 288-1ap (*Australopithecus afarensis*, ca. 20%),
761 IPS18800.28 (*Hispanopithecus laietanus*, ca. 17% [IPS18800.28_1] and ca. 20%
762 [IPS18800.28_2]), RUD 184 (*Rudapithecus hungaricus*, ca. 20%), and in four (μ)XCT-based
763 subsamples representing *Homo sapiens* (*Homo* in the pink space), *Pan*, *Gorilla* and *Pongo* (both
764 15% and 20% cross-sectional contours). TM 266-01-063 is represented by two reconstructed
765 outlines approximating its most likely original shape (TM 266-01-0631_1 and TM 266-01-
766 063_2; SOM Fig. 4).

767

768 **Figure 6.** The partial femur TM 266-01-063 (left) in anterior (a), posterior (b), medial (c), and
769 lateral (d) views compared to the CT-based reconstruction of BAR 1002'00 (Puymerail, 2011,
770 2017, based on a record kindly made available by B. Senut and M. Pickford). Technical
771 characteristics of the CT-record are detailed in Galik et al. (2004); for additional 3D projections
772 of BAR 1002'00, see also Kuperavage et al. (2018). Scale bar = 2 cm.

773



a



b

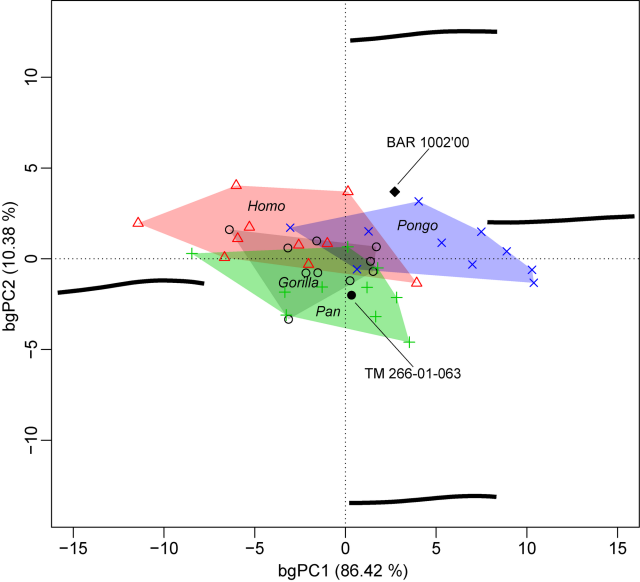


c



d

a**b****c**



TM 266-01-063

human

Pan

Gorilla

Pongo

15%

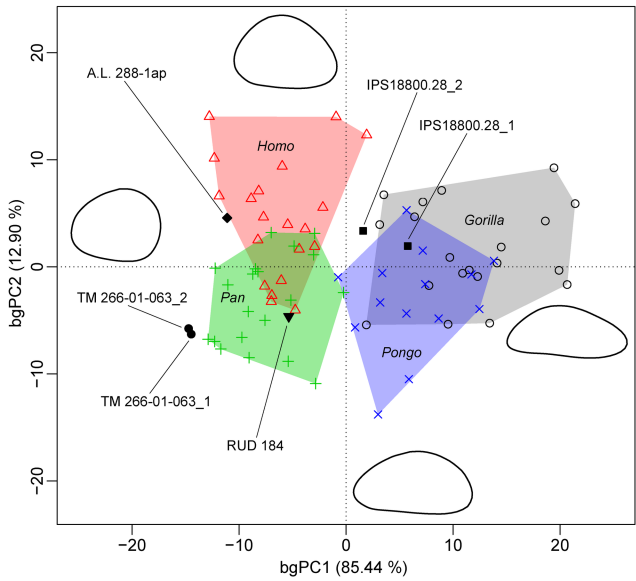
M

F

M

F







a



b



c



d

Table 1

Measurements of TM 266-01-063 (*Sahelanthropus tchadensis*) compared with BAR 1002'00 and BAR 1003'00 (both *Orrorin tugenensis*) and with samples representing australopiths (*Australopithecus* and *Paranthropus*), modern humans (*Homo sapiens*) and extant great apes (*Pan*, *Gorilla*, *Pongo*). For each comparative sample we provide the mean \pm SD, range, and sample size.

| Variable | TM 266- 01-63 | BAR 1002'00 | BAR 1003'00 | Australopiths (<i>n</i> = 16) | <i>H. sapiens</i> (<i>n</i> = 94) | <i>Pan</i> (<i>n</i> = 63) | <i>Gorilla</i> (<i>n</i> = 57) | <i>Pongo</i> (<i>n</i> = 5) |
|------------------------------------|------------------|----------------|----------------|-----------------------------------|---------------------------------------|---|---|--|
| Sub-trochanteric m-l diam. (mm) | 31.6 | 25.7 | 27.3 | 29.5 \pm 4.9 23.5–38.9 | 32.5 \pm 2.4 27.4–38.3 | 27.6 \pm 2.2 23.5–34.0 | 38.6 \pm 4.6 29.3–45.9 | 23.4 \pm 4.2 19.3–30.1 |
| Subtrochanteric a-p diam. (mm) | 25.3 | 20.4 | 22.0 | 22.2 \pm 4.0 16.9–29.6 | 24.1 \pm 2.5 18.7–30.8 | 23.4 \pm 1.6 20.5–27.8 | 32.5 \pm 4.1 24.7–39.3 | 19.3 \pm 1.8 16.6–21.0 |
| Platymeric index (%) | 80.1 | 79.4 | 80.6 | 74.6 \pm 3.7 66.4–81.5 | 74.3 \pm 6.6 60.6–88.9 | 85.3 \pm 5.8 71.1– (<i>n</i> = 63) | 84.3 \pm 5.1 76.5– (<i>n</i> = 57) | 83.3 \pm 8.8 69.6–91.9 (<i>n</i> = 5) |

| | | | | | | | | |
|----------------------------|-------------------|------|------|--------------------------------------|---|---|---|---|
| Midshaft m-l diam. (mm) | 28.3 ^a | 25.5 | 26.3 | 24.7±2.4 21.9–27.8 (n = 4) | 26.0±1.9 21.1–31.1 (n = 94) | 25.7±2.2 21.4–29.2 (n = 21) | 41.3±3.9 32.8–46.6 (n = 10) | 22.0±3.9 17.9–27.9 (n = 5) |
| Midshaft a-p diam. (mm) | 26.2 ^a | 20.8 | 21.3 | 22.9 ± 2.0 21.0–25.0 (n = 3) | 27.0 ± 2.7 21.7–33.5 (n = 94) | 24.5 ± 2.3 21.4–30.1 (n = 21) | 33.6 ± 2.7 26.9–36.2 (n = 10) | 19.2 ± 2.5 16.1–23.1 (n = 5) |
| Pilastric index (%) | 92.6 | 81.6 | 81.0 | 93.1 89.9–95.9 (n = 3) | 104.1 ± 9.3 88.3– 128.0 (n = 94) | 95.5 ± 6.8 83.3– 109.6 (n = 21) | 81.6 ± 4.3 73.8–88.0 (n = 10) | 87.5 ± 6.2 79.6–94.5 (n = 5) |
| Neck-shaft angle (°) | >135 ^b | 124 | - | 119.3 ± 4.7 112.5–125 (n = 11) | 127.4 ± 4.1 113.3– 136.3 (n = 96) | 123.1 ± 5.1 109.3– 133.3 (n = 66) | 118.9 ± 5.1 106.0– 129.0 (n = 83) | 134.0 ± 5.2 127.3– 145.1 (n = 18) |

Abbreviations: m-l = mediolateral; a-p = anteroposterior.

^a Measured at the point of maximum anteroposterior curvature as seen in medial and lateral views (see SOM Fig. S2).

^b See SOM Figure S1.